KSHV dysregulates bulk macroautophagy, mitophagy and UPR to promote endothelial to mesenchymal transition and CCL2 release, key events in viral-driven sarcomagenesis.

Roberta Santarelli[1], Ana Maria Brindusa Arteni[1], Maria Saveria Gilardini Montani[1], Maria Anele Romeo[1], Aurelia Gaeta[2], Roberta Gonnella[1], Alberto Faggioni[1] and Mara Cirone[1, 3]

[1] Department of Experimental Medicine, La Sapienza University of Rome, Viale Regina Elena 324, 00185, Rome, Italy; Laboratory Affiliated to Istituto Pasteur Italia-Fondazione Cenci Bolognetti, Rome, Italy.

[2] Department of Molecular Medicine, Sapienza University of Rome, Rome, Italy.

[3] Corresponding author. Electronic address: mara.cirone@uniroma1.it.

What's New

The oncogenic gammaherpesvirus KSHV is present in almost all 100% of Kaposi Sarcoma (KS) lesions of all subtypes and is considered the causative agent of KS. Here the authors studied the KSHV-mediated transformation of HUVEC into spindle cells, which closely resemble KS cells, as a model of viral-induced sarcomagenesis. They unveiled that autophagy and mitophagy reduction by KSHV promoted EndMT and activated ERstress/UPR that in turn induced inflammation and contributed to EndMT.

This article has been accepted for publication and undergone full peer review but has not been through the copyediting, typesetting, pagination and proofreading process which may lead to differences between this version and the Version of Record. Please cite this article as doi: 10.1002/ijc.33163

Key words CCCP, EndMT, HUVEC, KSHV, Macroautophagy, Metformin, Mitophagy, PERK, RAB7, SNAI1.

Abbreviations

α-SMA: actin alpha 2, smooth muscle; ACTB: actin beta; AMPK: protein kinase AMP-activated catalytic subunit alpha 2; ATF4: activating transcription factor 4; Baf: bafilomycin A_1; CCL2: C-C motif chemokine ligand 2; CCCP: Carbonyl cyanide 3-chlorophenylhydrazone; GADD153 /CHOP: DNA damage inducible transcript 3; GAPDH glyceraldehyde-3-phosphate dehydrogenase; GRP78/BiP: heat shock protein family A (Hsp70) member 5; eIF2a: eukaryotic translation initiation factor 2 subunit alpha; 4EBP1: eukaryotic translation initiation factor 4E binding protein 1; HADHA: hydroxyacyl-CoA dehydrogenase trifunctional multienzyme complex subunit alpha; IL6: interleukin 6; LC3: microtubule associated protein 1 light chain 3; LMNB: lamin B; MFN2: mitofusin 2; MTOR: mechanistic target of rapamycin kinase; NF-kB: nuclear factor kappa-light-chain-enhancer of activated B cells; NRF2: nuclear factor erythroid 2 like 2; PECAM1/CD31: platelet and endothelial cell adhesion molecule 1; PERK: eukaryotic translation initiation factor 2 alpha kinase 3; PIK3CA: phosphatidylinositol-4,5-bisphosphate 3-kinase catalytic subunit alpha; SQSTM1: Sequestosome 1; ULK1: unc-51 like autophagy activating kinase 1; UPR: Unfolded Protein Response; TUBA1A: tubulin; VEGFA: vascular endothelial growth factor A; VE-cadherin: Vascular endothelial cadherin; ZEB1: zinc finger E-box binding homeobox 1.

Abstract

Kaposi's Sarcoma-associated Herpesvirus (KSHV) is the causative agent of KS, an aggressive neoplasm that mainly occurs in immune-compromised patients. Spindle cells represent the main feature of this aggressive malignancy and arise from KSHV-infected endothelial cells undergoing endothelial to mesenchymal transition (EndMT), which changes their cytoskeletal composition and organization. As in epithelial to mesenchymal transition (EMT), EndMT is driven by transcription factors such as SNAI1 and ZEB1 and implies a cellular reprogramming mechanism regulated by several molecular pathways, particularly PI3K/AKT/MTOR. Here we found that KSHV activated MTOR and its targets 4EBP1 and ULK1 and reduced bulk macroautophagy and mitophagy to promote EndMT, activate ER stress/ Unfolded Protein Response (UPR), and increase the release of the pro-angiogenic and pro-inflammatory chemokine CCL2 by HUVEC cells. This study suggests that the manipulation of macroautophagy, mitophagy, and UPR and the interplay

between the three could be a promising strategy to counteract EndMT, angiogenesis, and inflammation, the key events of KSHV-driven sarcomagenesis.

Introduction

Kaposi's Sarcoma-associated Herpesvirus (KSHV), a virus belonging to gammaherpesvirus family, is strongly involved in the pathogenesis of Primary Effusion Lymphoma (PEL) and is the causative agent of Kaposi's Sarcoma (KS). KS is an angio-proliferative neoplasm that exists in four different forms that share characteristic features of inflammation, intense angiogenesis, and abnormal proliferation in KSHV-infected spindle-shaped endothelial cells that arise from line blood or lymphatic vessels[1]. All these processes are sustained by pro-inflammatory cytokines such as interleukin 6 (IL6) and chemokines such as IL8 and CCL2 that also play a role in the recruitment of an abundant leucocyte infiltrate in the tumor bed of KS lesions[2]. Although KSHV *in vitro* infection of endothelial cells (HUVEC) does not lead to a full neoplastic transformation, the virus is able to change them into spindle cells closely resembling KS cells. Therefore, HUVEC transformation represents an interesting model to study KSHV-driven tumorigenesis to which oncogenic viral proteins, ROS, and the activation of multiple cellular pathways contribute.

A central role is played by PI3K/AKT/MTOR, which induces angiogenesis and resistance to apoptosis by increasing the production of the vascular endothelial growth factor (VEGF)[3] essential for the survival and growth of KS. MTOR also contributes to vasculogenesis by promoting the production of ROS, which may increase the permeability of KSHV-infected endothelial cells[4] and induce several other pro-tumorigenic effects crucial for viral tumorigenesis and tumor progression, such as the Warbourg effect[5], and endothelial to mesenchymal transition (EndMT)[6]. As in epithelial

to mesenchymal transition (EMT), cells undergoing EndMT acquire mesenchymal markers and properties that cause them to lose polarity and phenotypic/functional characteristics. During such cellular reprogramming, cells down-regulate the expression of platelet and endothelial cell adhesion molecule 1 (PECAM1) and vascular endothelial cadherin (VE-cadherin) and up-regulate the expression of α-smooth muscle actin (α-SMA)[7]. The most important transcription factors that drive such cellular reprogramming are SNAI1, TWIST1, and zinc finger E-box binding homeobox 1 (ZEB1), a protein family that may either initiate and maintain EMT or EndMT[8].

EMT is strongly inter-connected to macroautophagy, a catabolic route essential for the maintenance of cellular homeostasis, as both autophagy and EMT play a pivotal role in the control of carcinogenesis[9] and are regulated by common molecular pathways including PI3K/AKT/MTOR. Interestingly, autophagy has been shown to counteract EMT by contributing to the degradation of SNAI1[10] and SNAI1 may be up-regulated by the autophagic protein Sequestosome 1 (SQSTM1) through the activation of nuclear factor kappa-light-chain-enhancer of activated B cells (NF-kB)[11]. Although MTOR is the master regulator of macroautophagy, whether its activation by KSHV in endothelial cells[3] could lead to bulk or selective macroautophagy reduction and if such effects promote EndMT or the other features of KS remain to be explored. Additionally, macroautophagy is strongly interconnected with endoplasmic reticulum (ER) stress and Unfolded Protein Response (UPR)[12] and the latter has been previously reported to promote EMT[13] or up-regulate SNAI1[14] by inducing the Ser-9 de-phosphorylation of GSK3 beta[15].

UPR activation is orchestrated by IRE1 alpha, eukaryotic translation initiation factor 2 alpha kinase 3 (PERK), and activating transcription factor 6 (ATF6) and activates several processes, including autophagy, in an attempt to relieve cells from ER stress[16]. KSHV infection of endothelial

cells has been reported to up-regulate ATF4, a UPR molecule activated downstream of PERK, leading to an increased release of CCL2[17], which may inhibit autophagy[18] or up-regulate the expression of SQSTM1 [19]. Based on this knowledge, in this study we investigated whether KSHV could exploit the intricate connections between bulk and selective macroautophagy and UPR to promote EndMT and angiogenesis in HUVEC cells. We also explored the possibility to counteract KSHV-driven pro-tumorigenic effects by restoring macroautophagy and mitophagy with Metformin (Met), an anti-diabetic drug able to stimulate macroautophagy[20], Carbonyl cyanide 3-chlorophenylhydrazone (CCCP)[21], a mitophagy inducer, and GSK2606414, an inhibitor of the PERK branch of UPR.

MATERIALS AND METHODS

HUVEC cells and viral stock

Primary HUVEC cells (ScienCell, 8000) were cultured in endothelial cell medium (ECM, ScienCell, 1001) containing endothelial cell growth supplements (ECGS, ScienCell, 0025+1052+0503). For split cultures, HUVEC cells were trypsinized after they reached 80-90% confluence. Cells were grown at 37°C and 5% CO_2 in a humidified incubator. All experiments were performed with mycoplasma-free HUVEC cells.

Each aliquot of KSHV stock contained ~9×10^6 viral DNA copies/100 μl [53] in serum-free ECM, as measured by real-time DNA PCR (Nanogen Advanced Diagnostics, Milan, Italy), using primers amplifying the KSHV capsid protein gene, as previously described [55].

HUVEC infection and treatments

HUVEC cells were seeded at 4×10^5/ml in 6 well plates the day before infection and subsequently infected with $\sim 9 \times 10^6$ viral DNA copies/well. After 72hrs, LANA latent gene expression was used to monitor KSHV infection by western blotting analysis.

HUVEC cells were pretreated for 45 minutes with either metformin (Met, 3mM, Sigma Aldrich D150659), carbonyl cyanide 3-chlorophenylhydrazone (CCCP, 5μM, Sigma Aldrich C2759), or PERK inhibitor GSK2606414 (GSK, 100nM, Sigma Aldrich 516535). Bafilomycin A_1 (Baf, 15nM, Santa Cruz Biotechnology sc-201550), an inhibitor of vacuolar-H^+-ATPase, was added during the last 4 hours of infection. DMSO was added to untreated cells as a control.

Antibodies

The following antibodies were used as loading controls: rat monoclonal anti-LANA-1 antibody (Advanced Biotechnologies Inc., 13-210-100), rabbit polyclonal anti-LC3B (Novus Biologicals, NB 100-222055), mouse monoclonal anti-SQSTM1/p62 (BD Transduction Laboratories, 610833), rabbit monoclonal anti-SNAI1(Cell Signaling, 3879), rabbit polyclonal anti-RAB7 (1:500; Santa Cruz Biotechnology, sc-10767), rabbit polyclonal anti-phospho-MTOR (Ser2448) (1:500) (Cell Signaling, 5536), rabbit polyclonal anti-MTOR (Cell Signaling, 2983), rabbit polyclonal anti-phospho-4EBP1 (Thr37/46) (Cell Signaling, 2855), rabbit polyclonal anti-4EBP1 (Cell Signaling, 9452), mouse monoclonal anti-HADHA (Santa Cruz Biotechnology, sc-3744497), mouse monoclonal anti-MFN2 (Santa Cruz Biotechnology, sc-515647), mouse monoclonal anti-NRF2/NFE2L2 (Santa Cruz Biotechnology, sc-365949), mouse monoclonal anti-PECAM-1/CD31 (Santa Cruz Biotechnology, sc-69797), mouse monoclonal anti-VE-cadherin /VE-cadherin (Santa Cruz Biotechnology, sc-9989), mouse monoclonal anti-αSMA (Santa Cruz

Biotechnology, sc-53142), rabbit polyclonal anti-eIF2α (Cell Signaling, 2722), rabbit polyclonal anti-phospo-eIF2α (S51) (Cell Signaling, 3398), rabbit polyclonal anti-ZEB1 (Novus, NBP1-05987), rabbit monoclonal anti-GRP78/BiP (Cell Signaling, 3177), mouse monoclonal anti-GADD153/CHOP (Santa Cruz Biotechnology sc-7351), rabbit polyclonal anti-ULK1 antibody (Abcam, ab167139), rabbit phospho-ULK1 (Ser757) (Cell Signaling, 6888). Mouse monoclonal anti-ACTB/actin (SIGMA, A5441), mouse monoclonal anti-tubulin (SIGMA, T6199), goat anti-lamin B (Santa Cruz Biotechnology, sc-6216), and mouse monoclonal anti-GAPDH (Santa Cruz Biotechnology, sc-137179).

RAB7 knockdown by small interfering RNA (siRNA)

HUVEC cells were transfected with a specific *RAB7* siRNA (Santa Cruz Biotechnology, sc-29460) by using INTERFERin transfection reagent (Polyplus transfection, 409-01) according to the manufacturer's instructions. Briefly, HUVEC cells were seeded at $2x10^5$/ml in 6-well plates in ECM the day before transfection. Subsequently, 80 pmol of *RAB7* siRNA and 12 µl of INTERFERin were diluted in Opti-MEM medium (Life Technologies, 31985062) and added to the cells. At 72 h post-transfection, cells were lysed and protein extract was analyzed by western blotting. Control siRNA-A (Santa Cruz Biotechnology, sc-37007) was used as scrambled control.

Western blotting

HUVEC cells were washed twice with PBS and lysed in a modified RIPA buffer containing 150 mM NaCl, 1% NP-40 (Calbiochem, 492015), 50 mM Tris-HCl, pH 8, 0.5% deoxycholic acid (SIGMA, D-6750), 0.1% SDS (SERVA, 39575.02), 1% Triton X-100, and protease and

phosphatase inhibitors (SIGMA, S8830, S6508 and 450022). 10 μg of each protein extract was subjected to electrophoresis on 4–12% NuPage Bis-Tris gels (Life Technologies/Novex, NP0323) and transferred to nitrocellulose membranes (GE Healthcare Life science/Amersham, 10600002 Protran). The membranes were blocked in 1X PBS-0.1% Tween-20 (SIGMA, P1379) containing 3% BSA (SIGMA, A4503) and incubated with specific primary antibodies for 1 hour at RT or overnight at 4°C. After several washes in 1X PBS-0.1% Tween-20, the membranes were incubated with either goat anti-mouse, goat anti-rabbit, or goat anti-rat secondary antibodies conjugated to horseradish peroxidase (Santa Cruz Biotechnology, sc-2005, sc-2004 and 31470 ThermoFisher, respectively). Finally, specific signals were detected using an enhanced chemiluminescence kit (Advansta, K-12045-D20). Densitometric analysis was performed using ImageJ software.

Measurement of intracellular reactive oxygen species production

To measure reactive oxygen species (ROS) production, 2′,7′-dichlorofluorescein diacetate (DCFDA; Sigma D6883) was used. Briefly, $5x10^5$ HUVEC cells were mock- or KSHV-infected for 72hrs, washed with prewarmed PBS, and incubated at 37°C with 10 μM DCFDA for 15 min in PBS. Then, cells were washed and analyzed with a FACScalibur flow cytometer (BD, USA), using CELLQuest software (BD Biosciences, San Jose, CA, USA) and live cells were gated according to their forward scatter (FSC) and side scatter (SSC) properties. For each analysis, 10,000 events were recorded.

Chemiluminescent immunometric assay

Supernatants from HUVEC were pretreated with GSK2606414 (100nM) for 45 minutes, mock- or KSHV-infected for 72hrs and collected. CCL2 and IL6 were measured by Magnetic Luminex assay performed by R&D systems a Bio-Techne brand using a human premixed multi-analyte kit (R&D systems Bio-Techne, LXSAHM) according to the manufacturer's instructions.

Statistical analyses

All data are represented as the mean ± standard error of at least 3 independent experiments. The Student *t* test was used for statistical significance of the differences between treatment groups. Statistical analysis was performed using analysis of variance at 5% ($P < 0.05$).

Results

KSHV infection induces a time-dependent spindle cell morphology and EndMT reprogramming in HUVEC cells.

HUVEC cells were exposed to KSHV and, after 72 hours, infection was assessed by evaluating the expression of the viral protein LANA-1 by western blot analysis (Fig.1A), as this KSHV latent antigen has been previously reported to be expressed in these cells at this time post infection[22]. Next, whether viral infection could lead to the acquirement of a spindle cell phenotype, including the expression of a molecular pattern associated with EndMT, was evaluated. As shown in Fig.1B, we observed by optical microscopy that KSHV-infected HUVEC acquired a spindle-like morphology. Western blot analysis indicated that the expression levels of SNAI and ZEB1, transcription factors that play a pivotal role in EndMT, were up-regulated in KSHV-infected cells in comparison to the mock-infected cells (Fig.1C). Similarly, expression of the mesenchymal marker

α-smooth muscle actin (α-SMA) increased in infected cells (Fig.1C). These effects were observed 72 hours post-infection, while the down-regulation of the endothelial-specific proteins PECAM1/CD31 and VE-cadherin was observed at 6 days (Fig.1D). Of note, after 6 days post-infection, we also observed the formation of characteristic tubular vessels in the KSHV-infected HUVEC culture (Fig.1E). Together, these results suggest that KSHV infection induces a time dependent EndMT reprogramming in HUVEC cells.

KSHV infection activates MTOR and its targets 4EBP1 and ULK1 and reduces both bulk macroautophagy and mitophagy in HUVEC cells.

Reports have shown that the MTOR pathway promotes EndMT reprogramming[23] and can be activated by KSHV infection in endothelial cells[3]. Therefore, we assessed MTOR activation in KSHV-infected HUVEC cells and found that its phosphorylation, as well as that of its target 4EBP1, increased compared to mock-infected cells (Fig.2A and 2B). As MTOR is the master negative regulator of autophagy, we further investigated whether its activation is correlated to a reduction of bulk macroautophagy in these cells. To evaluate the autophagic flux, viral-infected and mock-infected HUVEC cells were either treated or not treated with Bafilomycin A_1 (Baf) and analyzed for the expression level of LC3I/II by western blot analysis. Baf is an inhibitor of vacuolar-H^+-ATPase that blocks the autophagic flux at the late stage, allowing the formation of the lapidated form of microtubule associated protein 1 light chain 3 (LC3II) to be evaluated, as it is either formed or degraded during autophagy activation[24]. As shown in Fig.2C, in presence of Baf, the expression level of LC3II was lower in infected cells compared to mock-infected cells, suggesting that KSHV infection reduced the basal macroautophagy in HUVEC cells. This effect

was then confirmed by the increased expression of SQSTM1 (Fig.2D), a protein degraded in a complete autophagic flux[24].

Among its targets, MTOR may phosphorylate unc-51-like kinase 1 (ULK1) at Ser757 residue and negatively affect mitophagy in addition to bulk macroautophagy[25,26]. Therefore, we evaluated ULK1Ser757 phosphorylation and mitophagy in KSKV- and mock-infected HUVEC. As shown in Fig.2E, ULK1Ser757 phosphorylation (pULK1) increased in the infected cells and concomitantly the expression level of the mitochondrial matrix protein hydroxyacyl-CoA dehydrogenase (HADHA), a protein mainly degraded during mitophagy, accumulated (Fig. 2F). These results suggest that both bulk macroautophagy and mitophagy were impaired by KSHV, which correlated to the activation of the MTOR pathway that has been reported to control both processes[27]. Finally, we found that the expression of mitofusin (MFN)2 increased following KSHV infection (Fig. 2G). MNF2 is a protein regulating mitochondrial fusion that is ubiquinated and degraded when mitophagy is induced[28], thus its accumulation further suggests that viral infection can lead to mitophagy dysregulation.

KSHV increases intracellular ROS and activates ER stress/UPR in infected HUVEC cells.

As bulk macroautophagy and particularly mitophagy play a pivotal role in the elimination of damaged mitochondria that are the main source of intracellular ROS, we evaluated ROS level in KSHV-infected HUVEC cells with reduced bulk macroautophagy and mitophagy. As shown in Fig.3A, intracellular ROS increased following viral infection as well as the expression of the anti-oxidant transcription factor nuclear factor erythroid 2 like 2 (NRF2) (Fig.3B). Given that ROS accumulation may trigger ER stress, we next investigated UPR activation in KSHV-infected cells.

We focused on the activation of PERK, the arm of UPR mainly involved in the regulation of ATF4 expression, as this transcription factor has been previously reported to be up-regulated by KSHV[17]. As shown in Fig.3C, pospho-eIF2α (peIF2α) expression increased following viral infection, suggesting that the PERK/eIF2α /ATF4 axis was activated by KSHV. Interestingly, UPR activation may decide cell death or survival depending on the expression of GADD153/CHOP (CHOP) and GRP78/BiP (BiP), the pro-death and pro-survival UPR molecules respectively. We assessed the expression of these molecules and found that CHOP expression was slightly affected by KSHV while BiP expression was highly increased in infected HUVEC cells (Fig.3D). Considering the pro-tumorigenic effects of KSHV, it is reasonable to expect the UPR to be skewed towards cell survival.

Macroautophagy and mitophagy dysregulation contributes to EndMT and UPR activation in infected HUVEC cells.

To assess the impact of reduced macroautophagy on UPR and EndMT, we performed a knock down of *RAB7* in HUVEC cells. As expected, by inhibiting the last steps of macroautophagy, *RAB7* silencing led to the accumulation of SQSTM1 and HADHA as well as increased expression of peIF2α and SNAI1 compared to the scramble-treated control (Fig.4A). These results suggest that the reduction of macroautophagy contributed to the activation of UPR and promoted EndMT similarly to EMT[29, 30]. Then we explored the possibility of interfering with EndMT reprogramming induced by KSHV by restoring macroautophagy with Metformin, a protein kinase AMP-activated catalytic subunit alpha 2 (AMPK) activator able to induce macroautophagy without interfering with the expression of KSHV latent proteins[31].

As shown in Fig. 4B, Metformin restored macroautophagy, as indicated by the reduction of SQSTM1, and counteracted SNAI1 up-regulation induced by KSHV, further suggesting the inter-connection between macroautophagy reduction and EndMT reprogramming in infected cells. To assess whether macroautophagy restoration by Metformin could reduce ER stress/UPR activation, we assessed the phosphorylation status of eIF2α in KSHV-infected cells. We found that Metformin reduced eIF2α phosphorylation (Fig.4C), confirming interplay between macroautophagy and ER stress/UPR activation in which macroautophagy helps rid cells of unwanted materials, leading to the exacerbation of ER stress when macroautophagy is reduced[32]. Additionally, we found that Carbonyl cyanide 3-chlorophenylhydrazone (CCCP), a drug known to stimulate bulk macroautophagy and trigger mitophagy[21], reduced SQSTM1, SNAIL1, reduced eIF2α phosphorylation and down-regulated HADHA (Fig. 4D), a mitochondrial protein mainly degraded through mitophagy[27] (Fig. 4E). These results confirm that the restoration of macroautophagy and mitophagy could help to counteract ER stress and EndMT induced by KSHV in HUVEC cells. Optical microscopy observations confirmed that both Met and CCCP prevented the infected HUVEC from acquiring spindle cell morphology (Fig. 4E).

PERK activation promotes the release of CCL2 and contributes to EndMT in KSHV-infected HUVEC cells.

It has been reported that KSHV-mediated activation of ATF4 promotes the release of the pro-inflammatory chemokine CCL2[17]. Based on our finding that KSHV activated the PERK-eIF2α-ATF4 axis in HUVEC, we assessed the release of CCL2 by the infected cells. Following viral infection, we observed an increased production of this chemokine that was reduced by inhibiting the

PERK arm of UPR by GSK2606414 (GSK) (Fig.5A). The production of the pro-inflammatory cytokine IL6, which increases in KSHV infection, was slightly affected by GSK (Fig.5A), suggesting that the production of IL6 is regulated by a different mechanism than CCL2. We further evaluated whether PERK activation could contribute to EndMT, which CCL2 has been reported to promote[33]. As shown in Fig.5B, GSK reduced SNAI1 expression, suggesting that UPR activation promoted sarcomagenesis by increasing the release of CCL2 and promoting EndMT reprogramming.

Discussion

Our results indicate that dysregulation of bulk macroautophagy, mitophagy and UPR by KSHV infection contributes to viral-induced EndMT reprogramming and angiogenesis in HUVEC cells (Fig.6). This may represent a new interesting link between the activation of MTOR and EndMT or angiogenesis induction by KSHV. The KSHV-mediated activation of MTOR has been previously reported to induce several pro-tumorigenic effects in endothelial cells, i.e. to sustain cell survival[3], promote the formation of the tumor vasculature typical of KS, and engage a cross-talk with Rac1, a molecule essential for vascular development [34] that both activates[35] and is activated by MTOR[36].

We show for the first time that MTOR activation correlated with bulk macroautophagy and mitophagy dysregulation and that such effects play an important role in KSHV-driven sarcomagenesis. The reduction of macroautophagy and particularly of mitophagy is known to promote tumorigenesis by leading to the accumulation of ROS-producing damaged mitochondria[37]. Given the strong interplay between macroautophagy/mitophagy and ER stress/UPR[32] mediated by

ROS accumulation, we found that in addition to reducing the macroautophagic processes, KSHV activated the PERK arm of UPR in infected HUVEC, promoting the release of CCL2, a chemokine strongly involved in angiogenesis in the course of KS[38]. Interestingly, PERK activation also promoted EndMT, possibly by increasing the production of CCL2 that may up-regulate SNAI1[33] and impair autophagy[19], or because UPR activation may increase SNAI1 expression through the Ser-9 de-phosphorylation and activation of GSK3 beta[15]. Our results replicate previous findings that KSHV up-regulates ATF4 and promotes CCL2 production[17] and as well as previous findings that show ER stress and PERK activation correlate with increased production of CCL2 in other cell types [39]. Among numerous effects, CCL2 may stimulate the release of Vascular Endothelial Growth Factor A (VEGFA)[40], cytokine that promotes EMT and recruits macrophages in the tumor bed of KS lesions, polarizing them into M2, alternatively activated macrophages that support cancer[41] by contributing to the angiogenic process[42]. Interestingly, KSHV is able to infect macrophages[43] and their recruitment could facilitate viral infection further promoting M2 polarization, as our recent studies suggest (Gilardini Montani et al. submitted).

Given that macrophages are the most representative leukocytes in KS lesions, the finding that KSHV adopts several strategies to skew their polarization into M2 elucidates a crucial event in viral-induced tumorigenesis. Furthermore, CCL2 may negatively regulate autophagy[18] or engage a cross-talk with SQSTM1 in which CCL2 activates MTOR and reduces autophagy, leading to an accumulation of SQSTM1 that promotes CCL2 transcription[19], in a positive feed-back loop essential for the angiogenesis and EndMT reprogramming necessary for KSHV-driven sarcomagenesis. Also SQSTM1 may up-regulate the expression of SNAI1[33, 44] and inhibit the degradation of TWIST1, another transcription factor that drives EMT[45]. Therefore, it appears that

vasculogenesis and EndMT are inter-connected processes strictly regulated by macroautophagy and UPR. Our findings suggest that the manipulation of macroautophagy, mitophagy, and UPR could represent a promising strategy to counteract KSHV-induced sarcomagenesis, as indicated by the reversion of viral-induced EndMT reprogramming by Metformin, an AMPK activator that restored autophagy and reduced ER stress. This anti-diabetes drug displays anticancer properties, including against KSHV-associated lymphomas[46], and has been shown to restrain EMT[47]. We also found that similarly to Metformin, CCCP, an autophagy and mitophagy inducer, partially prevented the KSHV-induced pro-tumorigenic effects. Previous findings have identified curcumin as a drug able to inhibit EMT and angiogenesis in lung cancer cells[48] with minimal toxic effects towards normal cells such as immune cells[49, 50], thus its ability to prevent KS-associated cancers may be interesting to assess. The restoration of macroautophagy as a strategy to counteract KSHV-driven tumorigenesis may be further encouraged by our previous findings that KSHV reduces autophagy to promote its replication [51, 52] and impair immune responses[53] and that similar effects are induced by Epstein-Barr virus (EBV) [51, 54] with which KSHV often cooperates to induce carcinogenesis.

Acknowledgments

We thank Prof. Danny Toomey (HHV6 foundation.org) for carefully editing the manuscript and Dr. Mariaignazia Carelli for technical assistance.

Disclosure of potential conflicts of interest

No potential conflicts of interest were disclosed.

Funding

This work was supported by grants from Istituto Pasteur Italia-Fondazione Cenci Bolognetti (49), PRIN 2017 (2017K55HLC) and by the Italian Association for Cancer Research (AIRC) Grant (IG 2019 Id.23040).

Data Accessibility

The data will be made available upon reasonable request

References

1. Cesarman E, Damania B, Krown SE, Martin J, Bower M, Whitby D. Kaposi sarcoma. *Nat Rev Dis Primers* 2019;**5**: 9.

2. Giffin L, Yan F, Ben Major M, Damania B. Modulation of Kaposi's sarcoma-associated herpesvirus interleukin-6 function by hypoxia-upregulated protein 1. *J Virol* 2014;**88**: 9429-41.

3. Wang L, Damania B. Kaposi's sarcoma-associated herpesvirus confers a survival advantage to endothelial cells. *Cancer Res* 2008;**68**: 4640-8.

4. Guilluy C, Zhang Z, Bhende PM, Sharek L, Wang L, Burridge K, Damania B. Latent KSHV infection increases the vascular permeability of human endothelial cells. *Blood* 2011;**118**: 5344-54.

5. Bhatt AP, Damania B. AKTivation of PI3K/AKT/MTOR signaling pathway by KSHV. *Front Immunol* 2012;**3**: 401.

6. Wang Z, Han Z, Tao J, Wang J, Liu X, Zhou W, Xu Z, Zhao C, Wang Z, Tan R, Gu M. Role of endothelial-to-mesenchymal transition induced by TGF-beta1 in transplant kidney interstitial fibrosis. *J Cell Mol Med* 2017;**21**: 2359-69.

7. Gasperini P, Espigol-Frigole G, McCormick PJ, Salvucci O, Maric D, Uldrick TS, Polizzotto MN, Yarchoan R, Tosato G. Kaposi sarcoma herpesvirus promotes endothelial-to-mesenchymal transition through Notch-dependent signaling. *Cancer Res* 2012;**72**: 1157-69.

8. Goossens S, Vandamme N, Van Vlierberghe P, Berx G. EMT transcription factors in cancer development re-evaluated: Beyond EMT and MET. *Biochim Biophys Acta Rev Cancer* 2017;**1868**: 584-91.

9. Chen HT, Liu H, Mao MJ, Tan Y, Mo XQ, Meng XJ, Cao MT, Zhong CY, Liu Y, Shan H, Jiang GM. Crosstalk between autophagy and epithelial-mesenchymal transition and its application in cancer therapy. *Mol Cancer* 2019;**18**: 101.

10. Zada S, Hwang JS, Ahmed M, Lai TH, Pham TM, Kim DR. Control of the Epithelial-to-Mesenchymal Transition and Cancer Metastasis by Autophagy-Dependent SNAI1 Degradation. *Cells* 2019;**8**.

11. Wang Y, Xiong H, Liu D, Hill C, Ertay A, Li J, Zou Y, Miller P, White E, Downward J, Goldin RD, Yuan X, et al. Autophagy inhibition specifically promotes epithelial-mesenchymal transition and invasion in RAS-mutated cancer cells. *Autophagy* 2019;**15**: 886-99.

12. Ogata M, Hino S, Saito A, Morikawa K, Kondo S, Kanemoto S, Murakami T, Taniguchi M, Tanii I, Yoshinaga K, Shiosaka S, Hammarback JA, et al. Autophagy is activated for cell survival after endoplasmic reticulum stress. *Mol Cell Biol* 2006;**26**: 9220-31.

13. Santamaria PG, Mazon MJ, Eraso P, Portillo F. UPR: An Upstream Signal to EMT Induction in Cancer. *J Clin Med* 2019;**8**.

14. Zheng H, Kang Y. Multilayer control of the EMT master regulators. *Oncogene* 2014;**33**: 1755-63.

15. Song L, De Sarno P, Jope RS. Central role of glycogen synthase kinase-3beta in endoplasmic reticulum stress-induced caspase-3 activation. *J Biol Chem* 2002;**277**: 44701-8.

16. Corazzari M, Gagliardi M, Fimia GM, Piacentini M. Endoplasmic Reticulum Stress, Unfolded Protein Response, and Cancer Cell Fate. *Front Oncol* 2017;**7**: 78.

17. Caselli E, Benedetti S, Grigolato J, Caruso A, Di Luca D. Activating transcription factor 4 (ATF4) is upregulated by human herpesvirus 8 infection, increases virus replication and promotes proangiogenic properties. *Arch Virol* 2012;**157**: 63-74.

18. Fang WB, Yao M, Jokar I, Alhakamy N, Berkland C, Chen J, Brantley-Sieders D, Cheng N. The CCL2 chemokine is a negative regulator of autophagy and necrosis in luminal B breast cancer cells. *Breast Cancer Res Treat* 2015;**150**: 309-20.

19. Xu W, Wei Q, Han M, Zhou B, Wang H, Zhang J, Wang Q, Sun J, Feng L, Wang S, Ye Y, Wang X, et al. CCL2-SQSTM1 positive feedback loop suppresses autophagy to promote chemoresistance in gastric cancer. *Int J Biol Sci* 2018;**14**: 1054-66.

20. Wang Y, Xu W, Yan Z, Zhao W, Mi J, Li J, Yan H. Metformin induces autophagy and G0/G1 phase cell cycle arrest in myeloma by targeting the AMPK/MTORC1 and MTORC2 pathways. *J Exp Clin Cancer Res* 2018;**37**: 63.

21. Ding WX, Ni HM, Li M, Liao Y, Chen X, Stolz DB, Dorn GW, 2nd, Yin XM. Nix is critical to two distinct phases of mitophagy, reactive oxygen species-mediated autophagy induction and Parkin-ubiquitin-p62-mediated mitochondrial priming. *J Biol Chem* 2010;**285**: 27879-90.

22. Cheng F, He M, Jung JU, Lu C, Gao SJ. Suppression of Kaposi's Sarcoma-Associated Herpesvirus Infection and Replication by 5'-AMP-Activated Protein Kinase. *J Virol* 2016;**90**: 6515-25.

23. Gao H, Zhang J, Liu T, Shi W. Rapamycin prevents endothelial cell migration by inhibiting the endothelial-to-mesenchymal transition and matrix metalloproteinase-2 and -9: an in vitro study. *Mol Vis* 2011;**17**: 3406-14.

24. Klionsky DJ, Abdelmohsen K, Abe A, Abedin MJ, Abeliovich H, Acevedo Arozena A, Adachi H, Adams CM, Adams PD, Adeli K, Adhihetty PJ, Adler SG, et al. Guidelines for the use and interpretation of assays for monitoring autophagy (3rd edition). *Autophagy* 2016;**12**: 1-222.

25. Tian W, Li W, Chen Y, Yan Z, Huang X, Zhuang H, Zhong W, Chen Y, Wu W, Lin C, Chen H, Hou X, et al. Phosphorylation of ULK1 by AMPK regulates translocation of ULK1 to mitochondria and mitophagy. *FEBS Lett* 2015;**589**: 1847-54.

26. Kim J, Kundu M, Viollet B, Guan KL. AMPK and MTOR regulate autophagy through direct phosphorylation of Ulk1. *Nat Cell Biol* 2011;**13**: 132-41.

27. Bartolome A, Garcia-Aguilar A, Asahara SI, Kido Y, Guillen C, Pajvani UB, Benito M. MTORC1 Regulates both General Autophagy and Mitophagy Induction after Oxidative Phosphorylation Uncoupling. *Mol Cell Biol* 2017;**37**.

28. Gegg ME, Cooper JM, Chau KY, Rojo M, Schapira AH, Taanman JW. Mitofusin 1 and mitofusin 2 are ubiquitinated in a PINK1/parkin-dependent manner upon induction of mitophagy. *Hum Mol Genet* 2010;**19**: 4861-70.

29. Catalano M, D'Alessandro G, Lepore F, Corazzari M, Caldarola S, Valacca C, Faienza F, Esposito V, Limatola C, Cecconi F, Di Bartolomeo S. Autophagy induction impairs migration and invasion by reversing EMT in glioblastoma cells. *Mol Oncol* 2015;**9**: 1612-25.

30. Grassi G, Di Caprio G, Santangelo L, Fimia GM, Cozzolino AM, Komatsu M, Ippolito G, Tripodi M, Alonzi T. Autophagy regulates hepatocyte identity and epithelial-to-mesenchymal and mesenchymal-to-epithelial transitions promoting Snail degradation. *Cell Death Dis* 2015;**6**: e1880.

31. Bareja A, Lee DE, White JP. Maximizing Longevity and Healthspan: Multiple Approaches All Converging on Autophagy. *Front Cell Dev Biol* 2019;**7**: 183.

32. Senft D, Ronai ZA. UPR, autophagy, and mitochondria crosstalk underlies the ER stress response. *Trends Biochem Sci* 2015;**40**: 141-8.

33. Zhuang H, Cao G, Kou C, Liu T. CCL2/CCR2 axis induces hepatocellular carcinoma invasion and epithelial-mesenchymal transition in vitro through activation of the Hedgehog pathway. *Oncol Rep* 2018;**39**: 21-30.

34. Tan W, Palmby TR, Gavard J, Amornphimoltham P, Zheng Y, Gutkind JS. An essential role for Rac1 in endothelial cell function and vascular development. *FASEB J* 2008;**22**: 1829-38.

35. Aslan JE, Tormoen GW, Loren CP, Pang J, McCarty OJ. S6K1 and MTOR regulate Rac1-driven platelet activation and aggregation. *Blood* 2011;**118**: 3129-36.

36. Saci A, Cantley LC, Carpenter CL. Rac1 regulates the activity of MTORC1 and MTORC2 and controls cellular size. *Mol Cell* 2011;**42**: 50-61.

37. Panigrahi DP, Praharaj PP, Bhol CS, Mahapatra KK, Patra S, Behera BP, Mishra SR, Bhutia SK. The emerging, multifaceted role of mitophagy in cancer and cancer therapeutics. *Semin Cancer Biol* 2019.

38. Caselli E, Fiorentini S, Amici C, Di Luca D, Caruso A, Santoro MG. Human herpesvirus 8 acute infection of endothelial cells induces monocyte chemoattractant protein 1-dependent capillary-like structure formation: role of the IKK/NF-kappaB pathway. *Blood* 2007;**109**: 2718-26.

39. Zhu S, Liu H, Sha H, Qi L, Gao DS, Zhang W. PERK and XBP1 differentially regulate CXCL10 and CCL2 production. *Exp Eye Res* 2017;**155**: 1-14.

40. Bonapace L, Coissieux MM, Wyckoff J, Mertz KD, Varga Z, Junt T, Bentires-Alj M. Cessation of CCL2 inhibition accelerates breast cancer metastasis by promoting angiogenesis. *Nature* 2014;**515**: 130-3.

41. Nakatsumi H, Matsumoto M, Nakayama KI. Noncanonical Pathway for Regulation of CCL2 Expression by an MTORC1-FOXK1 Axis Promotes Recruitment of Tumor-Associated Macrophages. *Cell Rep* 2017;**21**: 2471-86.

42. Low-Marchelli JM, Ardi VC, Vizcarra EA, van Rooijen N, Quigley JP, Yang J. Twist1 induces CCL2 and recruits macrophages to promote angiogenesis. *Cancer Res* 2013;**73**: 662-71.

43. Gregory SM, Wang L, West JA, Dittmer DP, Damania B. Latent Kaposi's sarcoma-associated herpesvirus infection of monocytes downregulates expression of adaptive immune response costimulatory receptors and proinflammatory cytokines. *J Virol* 2012;**86**: 3916-23.

44. Bertrand M, Petit V, Jain A, Amsellem R, Johansen T, Larue L, Codogno P, Beau I. SQSTM1/p62 regulates the expression of junctional proteins through epithelial-mesenchymal transition factors. *Cell Cycle* 2015;**14**: 364-74.

45. Qiang L, He YY. Autophagy deficiency stabilizes TWIST1 to promote epithelial-mesenchymal transition. *Autophagy* 2014;**10**: 1864-5.

46. Granato M, Gilardini Montani MS, Romeo MA, Santarelli R, Gonnella R, D'Orazi G, Faggioni A, Cirone M. Metformin triggers apoptosis in PEL cells and alters bortezomib-induced Unfolded Protein Response increasing its cytotoxicity and inhibiting KSHV lytic cycle activation. *Cell Signal* 2017;**40**: 239-47.

47. Han B, Cui H, Kang L, Zhang X, Jin Z, Lu L, Fan Z. Metformin inhibits thyroid cancer cell growth, migration, and EMT through the MTOR pathway. *Tumour Biol* 2015;**36**: 6295-304.

48. Jiao D, Wang J, Lu W, Tang X, Chen J, Mou H, Chen QY. Curcumin inhibited HGF-induced EMT and angiogenesis through regulating c-Met dependent PI3K/Akt/MTOR signaling pathways in lung cancer. *Mol Ther Oncolytics* 2016;**3**: 16018.

49. Pereira FV, Melo ACL, Low JS, de Castro IA, Braga TT, Almeida DC, Batista de Lima AGU, Hiyane MI, Correa-Costa M, Andrade-Oliveira V, Origassa CST, Pereira RM, et al. Metformin exerts antitumor activity via induction of multiple death pathways in tumor cells and activation of a protective immune response. *Oncotarget* 2018;**9**: 25808-25.

50. Masuelli L, Granato M, Benvenuto M, Mattera R, Bernardini R, Mattei M, d'Amati G, D'Orazi G, Faggioni A, Bei R, Cirone M. Chloroquine supplementation increases the cytotoxic effect of curcumin against Her2/neu overexpressing breast cancer cells in vitro and in vivo in nude mice while counteracts it in immune competent mice. *Oncoimmunology* 2017;**6**: e1356151.

51. Granato M, Santarelli R, Filardi M, Gonnella R, Farina A, Torrisi MR, Faggioni A, Cirone M. The activation of KSHV lytic cycle blocks autophagy in PEL cells. *Autophagy* 2015;**11**: 1978-86.

52. Cirone M. EBV and KSHV Infection Dysregulates Autophagy to Optimize Viral Replication, Prevent Immune Recognition and Promote Tumorigenesis. *Viruses* 2018;**10**.

53. Santarelli R, Granato M, Pentassuglia G, Lacconi V, Gilardini Montani MS, Gonnella R, Tafani M, Torrisi MR, Faggioni A, Cirone M. KSHV reduces autophagy in THP-1 cells and in differentiating monocytes by decreasing CAST/calpastatin and ATG5 expression. *Autophagy* 2016;**12**: 2311-25.

54. Gilardini Montani MS, Santarelli R, Granato M, Gonnella R, Torrisi MR, Faggioni A, Cirone M. EBV reduces autophagy, intracellular ROS and mitochondria to impair monocyte survival and differentiation. *Autophagy* 2019;**15**: 652-67.

55. Bigoni B, Dolcetti R, de Lellis L, Carbone A, Boiocchi M, Cassai E, Di Luca D. Human herpesvirus 8 is present in the lymphoid system of healthy persons and can reactivate in the course of AIDS. *J Infect Dis* 1996;**173**: 542-9.

Figure Legends

Figure 1. KSHV infection of HUVEC cells induces EndMT in a time-dependent manner. (A) HUVEC cells mock- (CT) or KSHV-infected (V) were analysed by western blotting analysis for the expression of viral latent protein LANA at 72 hrs post-infection; (B) optical microscopy analysis of KSHV infected (V) or mock-infected (CT) HUVEC cells; (C) SNAI1, ZEB1 and αSMA expression level as assessed by western blotting analysis on mock- (CT) or KSHV-infected (V) HUVEC cells

after 72 hrs; (D) western blotting showing the VE-cadherin and PECAM1 endothelial-specific proteins as well as αSMA expression in HUVEC cells mock- or KSHV-infected (V) after 6 days. (E) representative optical microscopy images of HUVEC cells 6 days post infection (V) or mock-infected (CT).

In the figure, ACTB, LMNB and GAPDH were used as loading controls and one representative experiment out of three is shown. The histograms represent the mean plus S.D. of the densitometric analysis of the ratio of LANA/ACTB, ZEB1/LMNB, SNAIL1/LMNB, αSMA/ACTB, VE-cadherin/LMNB, PECAM1/LMNB and αSMA/LMNB of three different experiments.

Figure 2. KSHV infection of HUVEC cells leads to MTOR pathway activation and macroautophagy and mitophagy impairment. Western blotting to assess the expression level of (A) pMTOR and its target (B) p4EBP1 in HUVEC cells mock- (CT) or KSHV-infected (V), cultured for 72 hrs; (C) the amount of the lipidated form of LC3 (LC3II) was determined by western blotting analysis of HUVEC cells mock- (CT) or KSHV-infected (V) after 72 hrs, in the presence or in the absence of Bafilomycin A_1 (Baf), added during the last 4hrs (CT+Baf and V+Baf); (D) SQSTM1 and (E) phospo-ULK1ser757 (pULK1) level in KSHV-infected (V) or mock-infected HUVEC cells after 72 hrs (CT); the effect of KSHV infection on mitophagy as assessed by western blotting analysis of (F) HADHA and (G) MFN2 proteins.

In the figure, LMNB, ACTB and GAPDH were used as loading controls and one representative experiment out of three is shown. The bands for the loading control LMNB in (A) and (C) are identical to those in Fig.1C, since all samples shown originate from the same gel/blot. Furthermore, the histograms represent the mean plus S.D. of the densitometric analysis of the ratio of

pMTOR/MTOR, MTOR/LMNB, p4EBP1/4EBP1, 4EBP1/ACTB, LC3II/GAPDH, SQSTM1/LMNB, pULK1/ULK1, ULK1/ATCB, HADHA/ATCB, MFN2/ACTB of three different experiments.

Figure 3. KSHV infection of HUVEC cells gives rise to an increase of intracellular ROS production and to ER stress/UPR-PERK arm activation. **(A)** FACS analysis of ROS production by HUVEC cells mock- (CT) or KSHV-infected (V) for 72 hrs, measured by DCFDA staining. The mean of fluorescence intensity is indicated. Solid grey peaks represent the isotype controls. One representative experiment of three is shown; (B) NRF2 level was evaluated in the same cells; (C) peIF2α and (D) CHOP and BiP expression level was assayed by western blotting on HUVEC mock- (CT) or KSHV-infected (V) after 72 hrs.

In the figure, ACTB was used as loading control and one representative experiment out of three is shown. Furthermore, the histograms represent the mean plus S.D. of the densitometric analysis of the ratio of NRF2/ATCB, peIF2α/eIF2α, eIF2α/ATCB, CHOP/ACTB and BiP/ACTB of three different experiments.

Figure 4. KSHV dysregulates macroautophagy and mitophagy to promote EndMT and UPR-PERK arm activation. (A) Western blotting to detect RAB7, SQSTM1, HADHA, peIF2α, eIF2α and SNAI1expression in HUVEC cells transfected for 72hrs with siRNA targeting *RAB7* gene or scramble siRNA (scr); (B) HUVEC cells were pretreated with DMSO or with metformin (Met, 3mM) for 45 min and subsequently KSHV- or mock-infected for further 72 hrs and analyzed by western blotting for SQSTM1 and SNAI1 or (C) peIF2α expression; (D) western blotting showing HADHA and SQSTM1 and SNAI1 or (E) peIF2α expression in HUVEC cells pretreated with

DMSO or with CCCP (5μM) for 45 min before KSHV-infection and analysed 72 hrs post-infection; (F) representative optical microscopy images of HUVEC cells pretreated with DMSO or with Met (3mM) or CCCP (5μM) for 45 min and then KSHV- (V) or mock-infected (CT) for further 72 hrs.

In the figure, ACTB and TUBA1A were used as loading control and one representative experiment out of three is shown. The bands for the loading control TUBA1A in (C) and in (B, right panel) are identical, since all samples shown originate from the same gel/blot. The histograms represent the mean plus S.D. of the densitometric analysis of the ratio of RAB7/ATCB, SQSTM1/ACTB, HADHA/ACTB, peIF2α/eIF2α, eIF2α/ATCB, SNAI1/ACTB or eIF2α/TUBA1A and SNAI1/ TUBA1A, of three different experiments.

Figure 5. CCL2 release by KSHV-infected HUVEC cells correlates with UPR-PERK arm activation. (A) CCL2 and IL6 release by KSHV- (V) or mock-infected HUVEC cells (CT) pre-treated or not with GSK 2606414 (GSK, 100nM) (GSK+V) as measured by Luminex assay. Mean plus SD of three different experiments is reported. * p value < 0.05; (B) the same samples were analyzed by western blotting for SNAI1expression level. ACTB was used as loading control and one representative experiment out of three is shown. Furthermore, the histograms represent the mean plus S.D. of the densitometric analysis of the ratio of SNAI1/ACTB of three different experiments.

Figure 6. Macroautophagy reduction by KSHV affects the interplay between EndMT, UPR and CCL2 release in infected HUVEC cells.

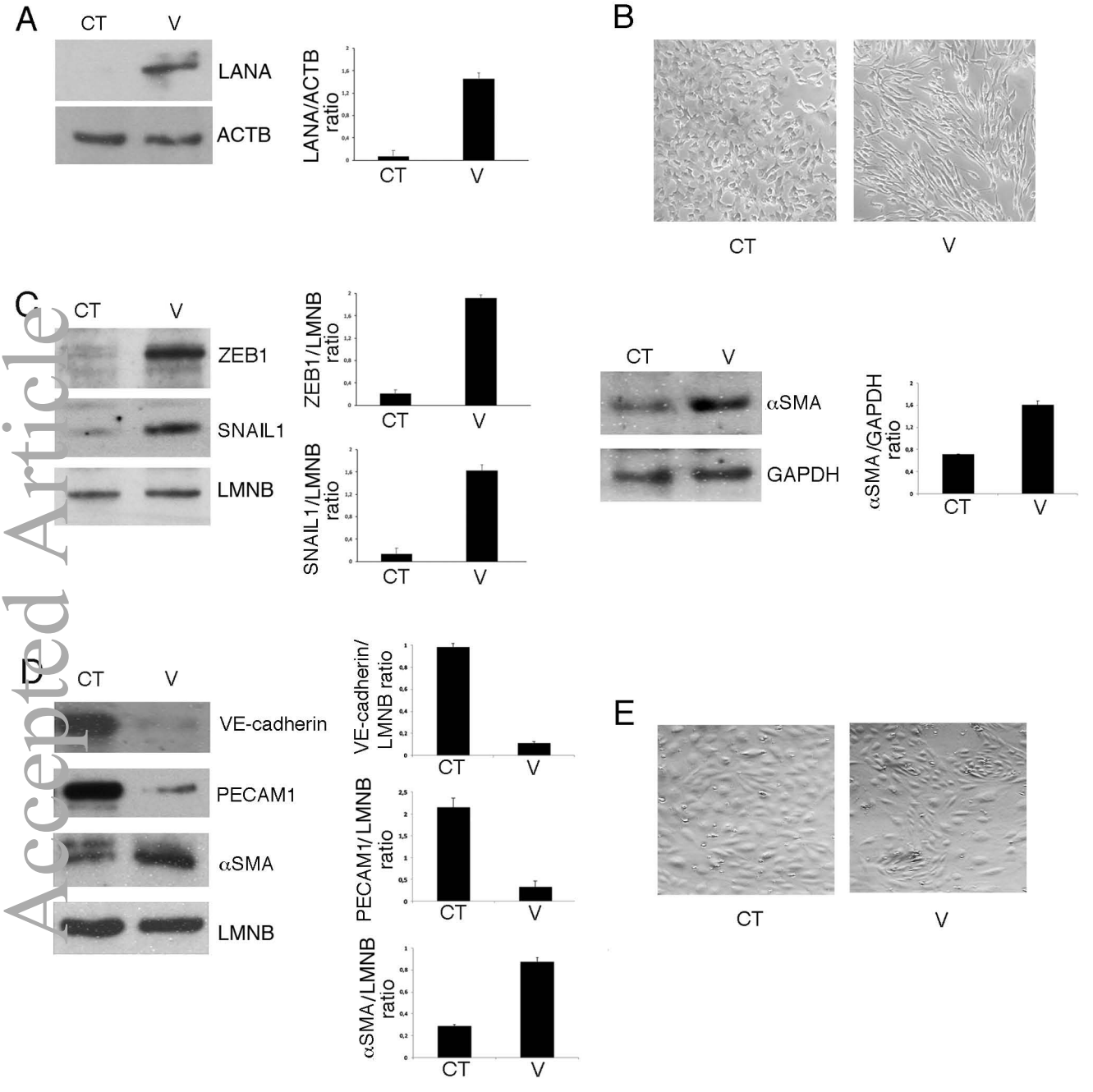

FIGURE 1

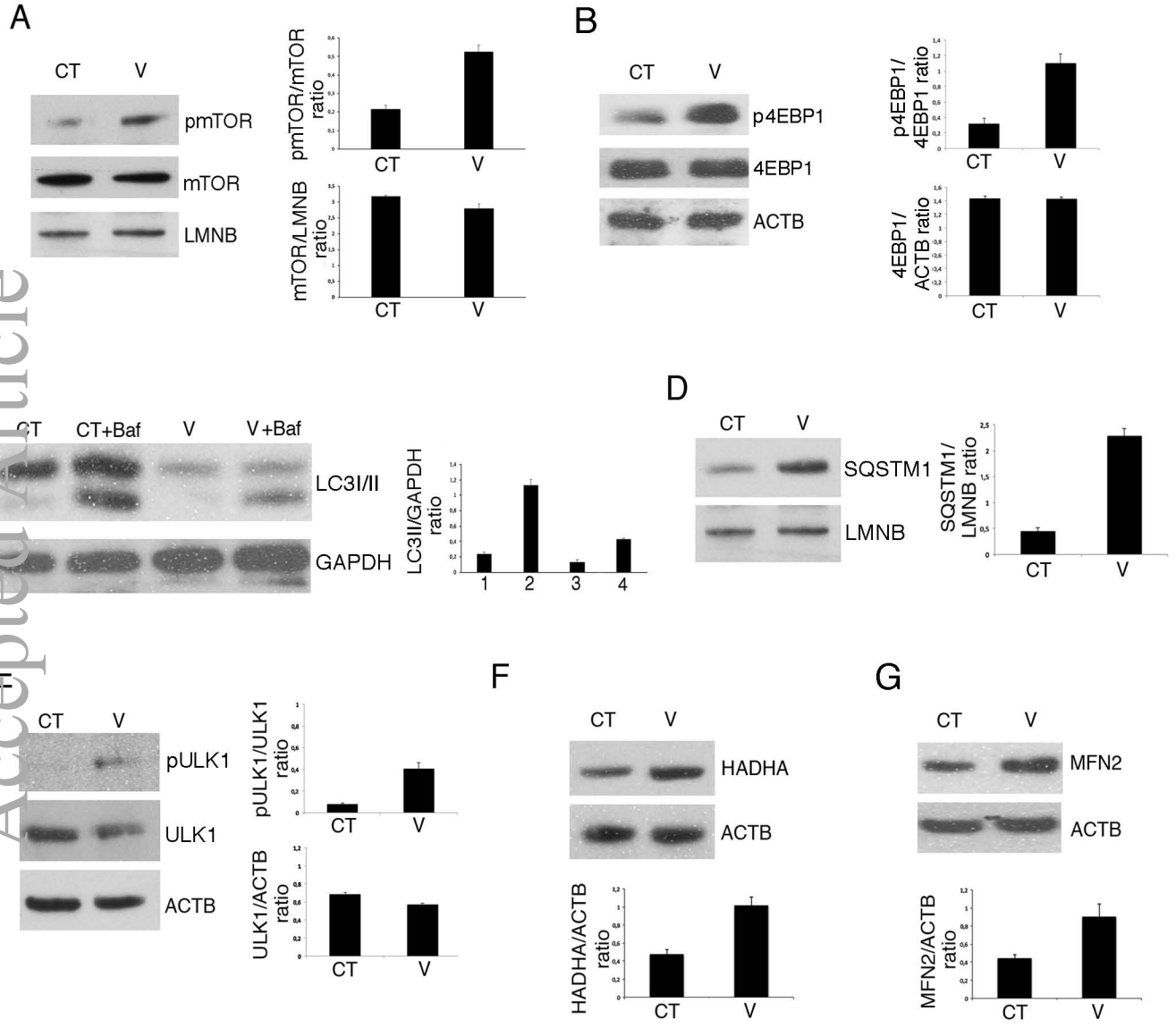

FIGURE 2

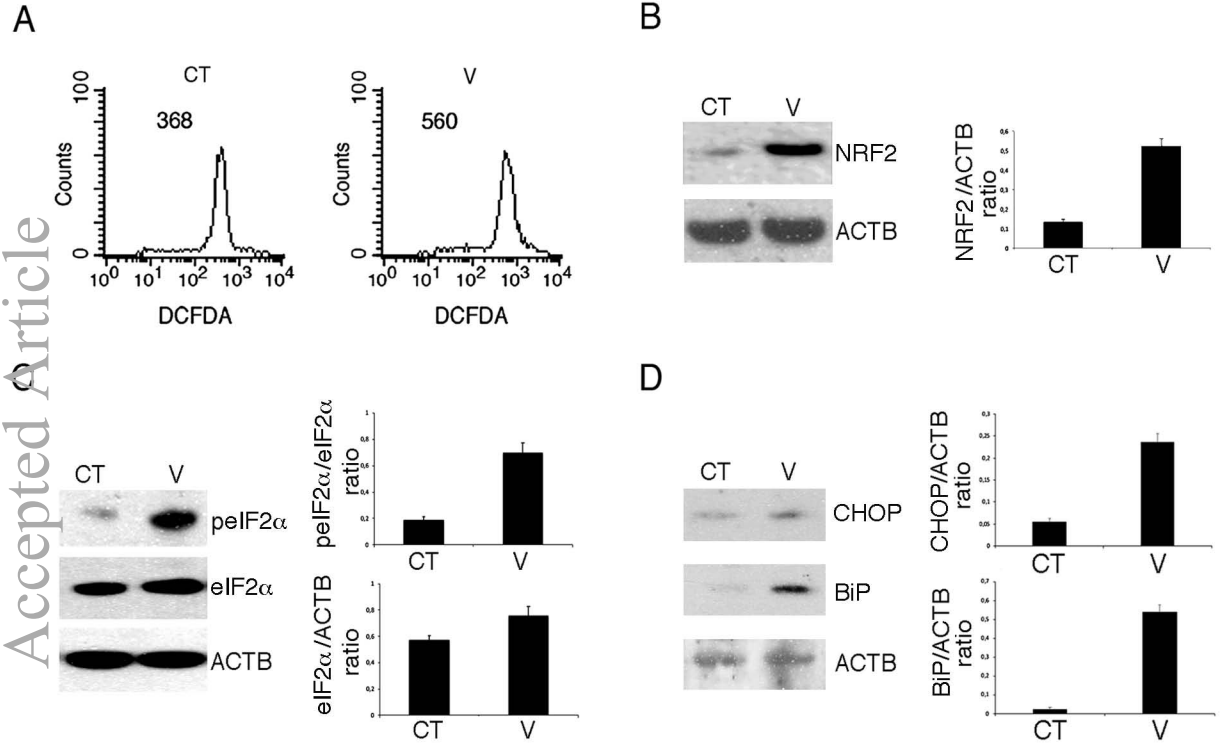

FIGURE 3

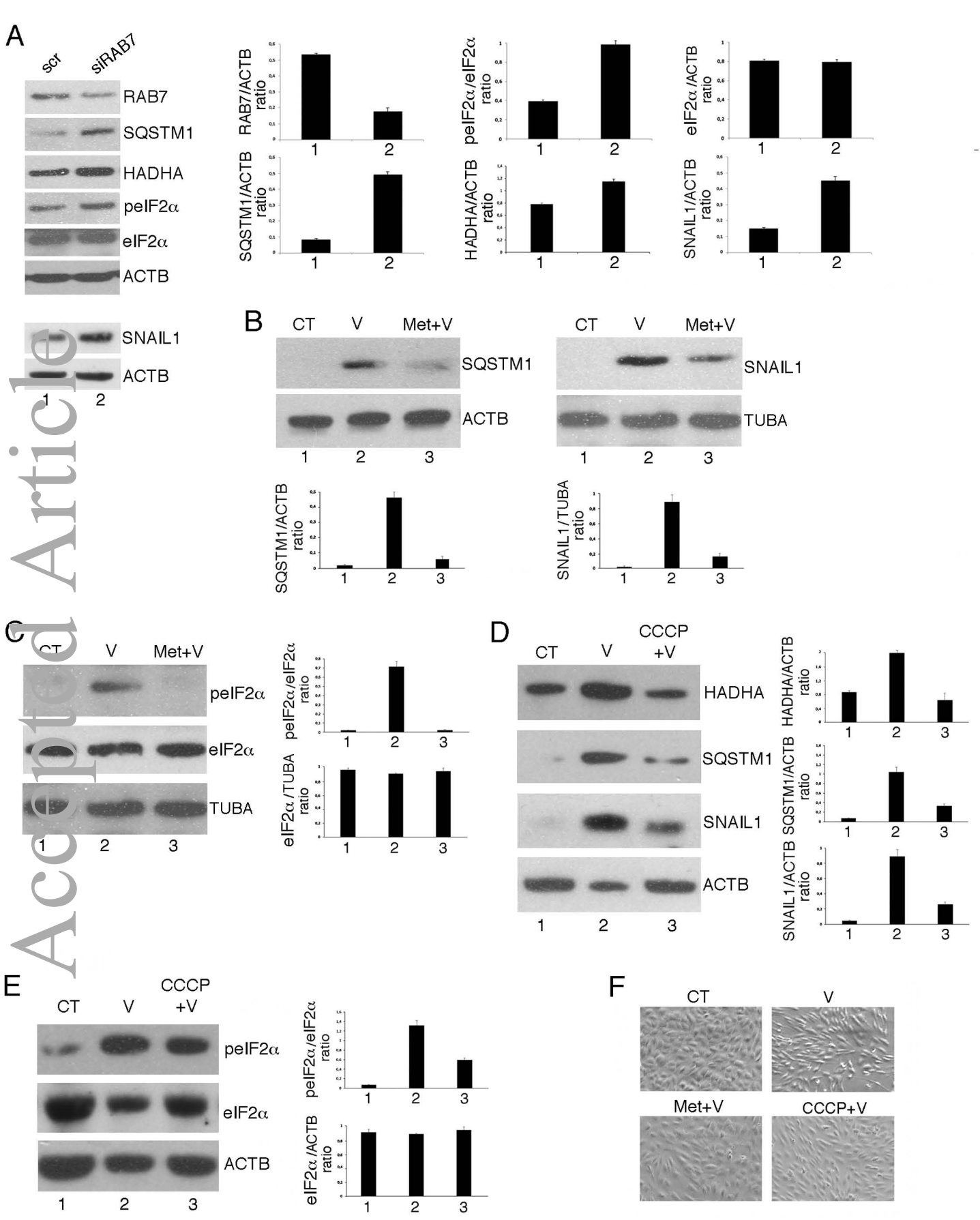

FIGURE 4

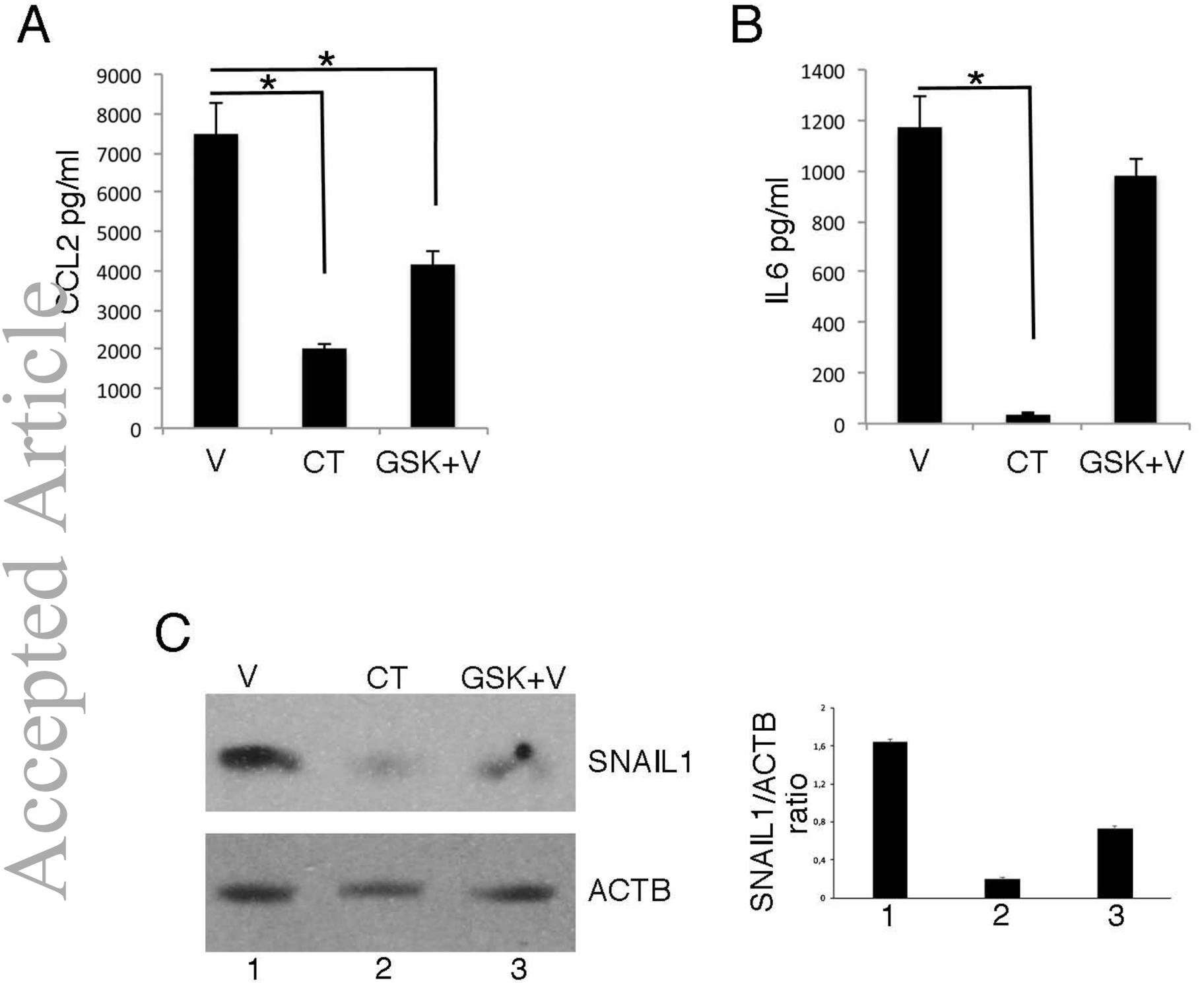

FIGURE 5

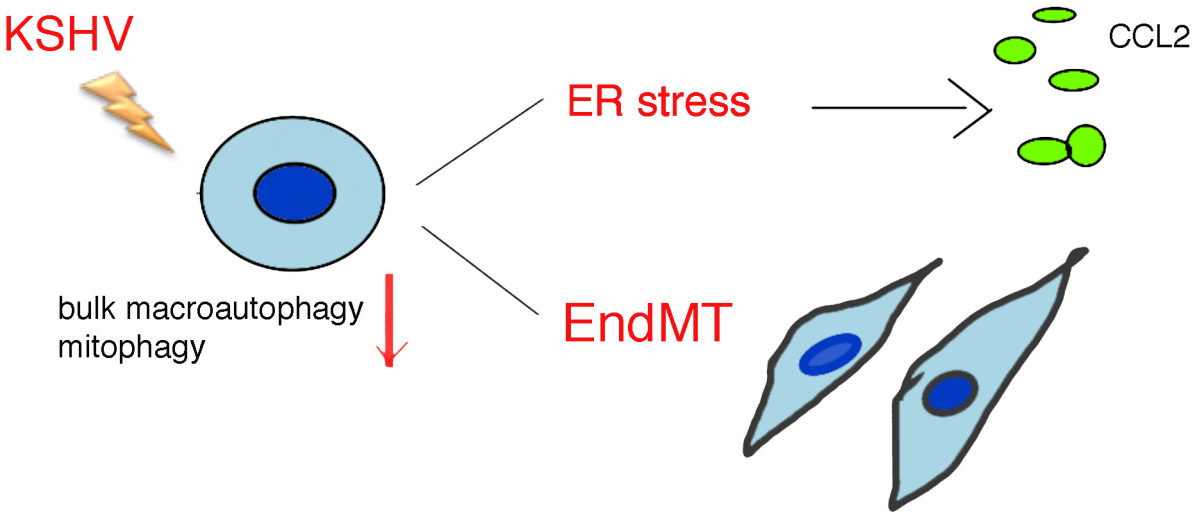

Figure 6